Memoirs of the Faculty of Engineering, Okayama University, Vol.40, pp.1-8, January, 2006

Fatigue Crack Propagation Behavior Bent from Precrack under Mixed-Mode Conditions

- Noting the Crack-Surface Contact due to a Compressive Residual Stress along a Precrack -

YouLi MA
The Graduate School of Natural Science and Technology, Okayama University
3-1-1 Tsushima-naka, Okayama, Japan

Kenichi SHIMIZU* and Tashiyuki TORII
Division of Industrial Innovation Sciences
The Graduate School of Natural Science and Technology, Okayama University
3-1-1 Tsushima-naka, Okayama, Japan

(Received December 12, 2005)

A testing for bent fatigue crack propagation under mixed-mode conditions was carried out using fatigue and annealed slant precracks with different slant angles, β , defined as the angle between loading and precrack directions in a rectangular plate. As a result, bent fatigue crack from the fatigue precrack with β =45deg. propagated under mixed-mode conditions with mode II stress intensity factor $(K_{II})_{est}$ evaluated from the discontinuous displacement measured along the crack. On the other hand, bent fatigue crack from the fatigue precrack with β =60deg. and from the annealed precracks with both slant angles of β =60deg. and β =45deg. propagated under the mode I behavior. This was because the compressive residual stress near the fatigue precrack caused contact to each other between the upper and the lower surfaces of the precrack with the smaller slant angle β . Furthermore, the fatigue crack propagation rates indicated almost the same relationship for all the data, using the mixed-mode effective stress intensity factor $(K_M)_{est}$, calculated from the discontinuous displacement measured along the bent fatigue crack.

1. INTRODUCTION

Fatigue crack initiation and propagation behaviors under mixed-mode conditions have to be studied for the fracture of materials subjected to loads in various directions. There are many reports on fatigue crack growth under the mixed-mode loading which have discussed a mechanical parameter controlling the crack growth direction (or the fracture angle) and the fatigue crack propagation rate [1-4]. Though such a mechanical parameter was probably affected by the crack surface contact due to the compressive residual stress around the crack, the bent fatigue crack propagation behavior were often discussed without the effects of the crack surface contact, such as bent cracks initiated from the slit and propagated under the positive mean stress [1-3] and it was reported that the crack deflection angle was determined by the amplitude of the cyclic loading regardless of the residual stress ahead the crack tip [4]. However, the concave and convex crack surface seems to contact frequently on a fatigue precrack with a compressive residual stress as the crack opening is suppressed. Therefore, it is probable that the effective stress intensity factors for mode I and mode II components are necessary to estimate based on the measured crack opening and sliding displacements for the mixed-mode fatigue crack propagation behavior under the various conditions. Nevertheless, the effective stress intensity factor for the mode II component have not been evaluated appropriately, while the effective stress intensity factor, K_{eff}, for the mode I component have been widely used [5].

In a previous paper [6], the author proposed a method of evaluating stress intensity factors, $\{(K_I)_{est}, (K_{II})_{est}\}$, from discontinuous displacements (opening for mode I, sliding for mode II) measured along a mixed-mode crack under tensile loading, which is considered as the effective stress intensity factor, $\{(K_I)_{eff}, (K_{II})_{eff}\}$, of mode I and II compo-

*E-mail: kshimizu@mech.okayama-u.ac.jp

This work is subjected to copyright.
All rights are reserved by this author/authors.

nent. In addition, using the $\{(K_I)_{est}, (K_{II})_{est}\}$ thus obtained, the effects of the compressive residual stress along a slant crack were investigated [7]. As a result, the discontinuous displacements along a slant crack and the resulting $\{(K_I)_{est}, (K_{II})_{est}\}$ values were decreased from their theoretical ones because of the contact between concave-convex crack surfaces due to the compressive residual stress.

In this study, using the $\{(K_I)_{est}, (K_{II})_{est}\}$ evaluated from the discontinuous displacement measured along a crack, the bent fatigue crack propagation rates and directions until the length of the bent crack length of about 0.6mm were discussed noting the crack surface contact due to the compressive residual stress along a precrack.

2. EXPERIMENTAL PROCEDURE

2.1 Specimen with a slant precrack

The material used here is medium carbon steel (S45C). The shape of the rectangular specimen with a slant precrack is shown in Fig. 1. As shown in the previous paper [6], the slant precrack specimen was prepared in the following manner. Using a servo-hydraulic fatigue testing machine, the precrack propagated under a mode I condition of push-pull sinusoidal wave loads at a speed of 20 Hz, a maximum stress σ_{max} = 140MPa, a stress ratio R = -1 till the crack initiation and R=0 after that. After the half -length of fatigue crack containing the radius of the notch reached about 3mm, the specimens were used as samples of fatigue cracks with residual stress. Some of them were annealed at 873 K for one hour and used as samples of annealed cracks without residual stress.

2.2 Measurement of residual stress

Residual stress toward the transverse direction to the slant precrack was measured using X-ray measurement method along the crack. X-ray conditions were as follows: Cr-K_α for a diffraction line, an X-ray radiation area of 1x1 mm^2, a half - value breadth method for determining the peak angle in a diffraction profile and a stress constant of -318.2MPa/deg.

2.3 Fatigue crack bent and growth testing

Using the same fatigue testing machine as that used to make the slant precrack, the bent fatigue crack was initiated and propagated near the slant precrack tip under a push-pull sinusoidal wave load at a speed of 20 Hz and a stress ratio R=0. The bent fatigue crack initiated from the slant precrack of β=60deg. was propagated with the maximum stress σ_{max}=100MPa. On the other hand, the maximum stress was increased to σ_{max}=120MPa for the specimen with the slant precrack of β=45deg. because the bent fatigue crack was not initiated with the maximum stress σ_{max}=100MPa. The length of bent fatigue crack, a', is defined as the distance between the bent fatigue crack tip and the slant precrack tip as indicated in Fig. 2. The bent fatigue crack was propagated to the length of a' 0.6 mm.

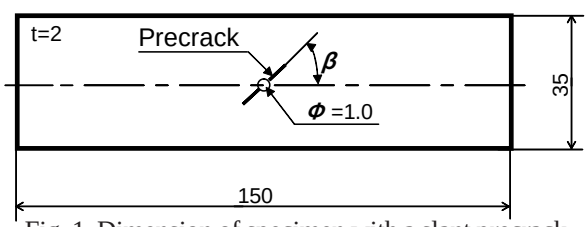

Fig. 1 Dimension of specimen with a slant precrack

2.4 Measurement of discontinuous displacement distribution

As shown in detail in the previous paper [8], discontinuous displacement distribution along a crack was measured as follows: a pair of micro-Vickers impressions marked longitudinally at a gage length of approximately 60 μm containing a crack line was spaced at 100 μm intervals along a slant crack. After the bent fatigue crack initiation, the fatigue testing was interrupted with every 100 μm crack propagation to mark additional pairs of micro-Vickers impressions spaced at 25 μm intervals along a bent crack. The displacements of these marks are measured in the directions of normal and parallel to the specimen before and after tensile loading using image processing system. From these values, crack opening discontinuous displacement V(=2v) and sliding discontinuous displacement U(=2u) are calculated based on geometric relation.

2.5 Measurement of fracture angles

Figure 2 shows the bent fatigue crack initiated from the precrack with a slant angle β=45deg.. The fracture angle, θ, was calculated from the angle BAC, in which the point A is the precrack tip, the point B is 200 μm behind from the precrack tip and point C is the bent fatigue crack tip determined at every 100 μm crack propagation.

3. EXPERIMENTAL RESULTS

3.1 Residual stress distribution around the precrack

Residual stress distributions around the precracks with slant angle β=45deg. are shown in Fig. 3. It can be seen that the compressive residual stress occurs near the fatigue precrack tip, while the residual stress along the annealed precrack is almost zero. The residual stress distribution around the fatigue and the annealed precracks with slant angle of β=60deg. are considered to be similar to those shown in Fig. 3 as both precracks with slant angles

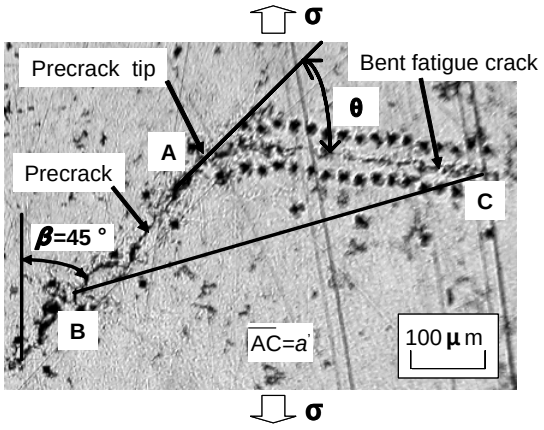

Fig. 2 Measurements of bent crack length and fracture angle

of β =60deg. and β =45deg. are propagated under the same mode I stress conditions.

3.2 Bent fatigue crack propagation

Fatigue crack propagation curves of bent fatigue cracks initiated from slant precracks are shown in Fig. 4. Bent fatigue cracks initiated from the annealed precrack propagate faster than those initiated from the fatigue precrack for both precracks with slant angle of β =60deg. and β =45deg.. On the other hand, bent fatigue cracks initiated from the precrack with slant angle of β =60deg. propagate faster than those initiated from the precrack with slant angle of β =45deg. though the maximum applied stress, σ_{max} is smaller for the specimen with a precrack of slant angle β =60deg. than that with a precrack of slant angle β =45deg. for both annealed precracks and fatigue precracks. The reason of this will be discussed in section 3.5.

3.3 Fracture angles

Change of fracture angles, θ_{mes}, with bent fatigue crack propagation is shown in Fig. 5. The fracture angles hardly change with bent fatigue crack propagation for all specimens. While the fracture angles obtained from the annealed precrack and the fatigue precrack are almost the same for the specimen with a slant precrack of β =60deg., the fracture angles obtained from the fatigue precrack are a little larger than those obtained from the annealed crack for the specimen with a slant precrack of β =40deg..

3.4 Discontinuous displacement distributions

Discontinuous displacement distributions obtained from the precracks with slant angle of β =60deg. and β =45deg. at the bent fatigue crack length of *a'* 0.2 mm are shown in Fig. 6. The horizontal axis, *r,* is the distance from the bent crack tip and it is defined by adding the length along the slant precrack behind the precrack tip. The crack opening displacement, *V,* and the crack sliding displacement, *U,* obtained from the fatigue precracks is smaller than those obtained from the annealed precrack on the slant precrack region for both specimens with the precrack of slant angle of β =60deg. and β =45deg.. It is considered that the sliding deformation is suppressed by the crack surface contact caused by the compressive residual stress around the slant precrack as mentioned in the previous paper [6]. Contrary to the crack opening displacement, the crack sliding displacements, *U,* on the bent fatigue crack initiated from the fatigue precrack are larger than those on the bent fatigue crack initiated from the annealed precrack for the specimen with the precrack of slant angle β =45deg.. As mentioned in the previous paper [8], the crack sliding displacements on the bent fatigue crack were almost zero for the relatively long bent crack initiated from slant cracks with various slant angles and various residual stress distributions. Conversely, large values of the crack sliding displacement are observed on the bent fatigue crack for the short bent crack as shown in Fig. 6(a), particularly for the slant precrack with a compressive residual stress. On the other hand, the crack sliding displacement on the bent crack are almost zero for both specimens with the annealed slant precrack and the fatigue slant precrack, while the crack opening displacements observed on the bent crack initiated from the fatigue slant precrack are smaller than those from the annealed one as indicated in Fig. 6(b).

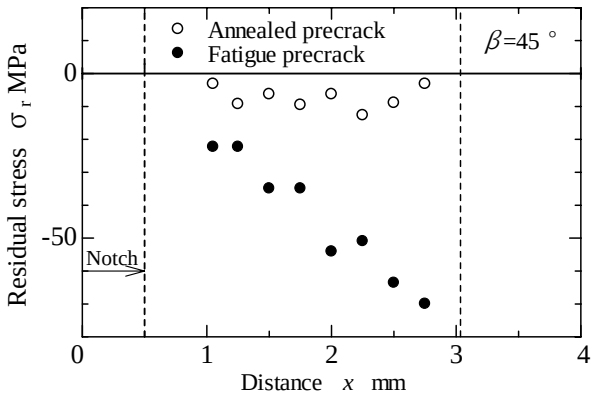

Fig. 3 X-ray residual stress distribution along a slant precrack

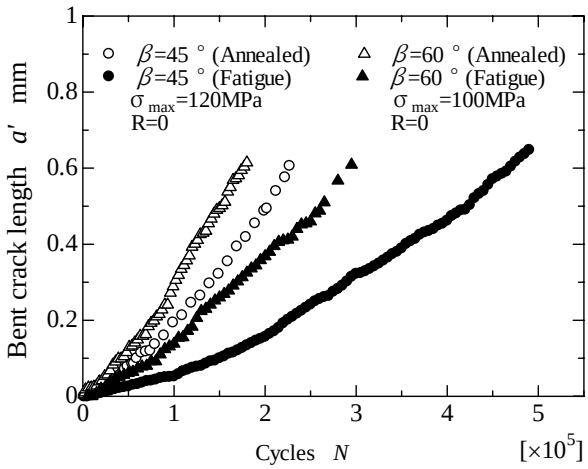

Fig. 4 Bent fatigue crack propagation curves

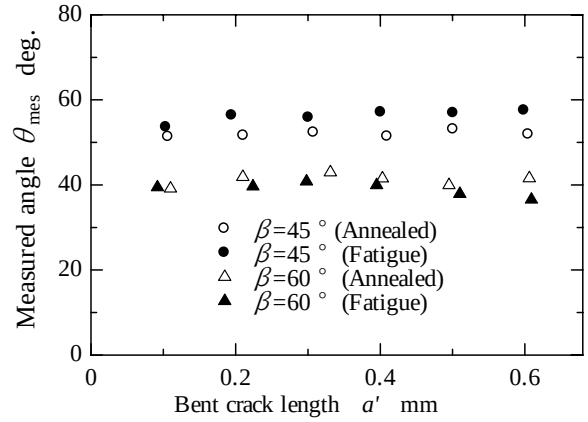

Fig. 5 Change of fracture angle with bent fatigue crack propagation

3.5 Stress intensity factors

Mode I and mode II stress intensity factors obtained from bent cracks, $(K_I)_{est}$ and $(K_{II})_{est}$, were calculated using a displacement extrapolation method of Eq. (1) under plane stress [9].

$$\begin{Bmatrix}(K_I)_{est}\\(K_{II})_{est}\end{Bmatrix}=\frac{E}{4}\lim_{r\to 0}\sqrt{\frac{2\pi}{r}}\begin{Bmatrix}V/2\\U/2\end{Bmatrix} \quad (1)$$

Here Young's modulus, E=205.8GPa, r is distance from bent crack tip. The stress intensity factors were calculated using the values of V and U obtained from the five points behind from the bent crack tip when the bent crack length was longer than 0.1mm. When the bent crack length was shorter than 0.1mm, the crack opening displacements and the crack sliding displacements on the slant precrack were transformed onto the assumed straight crack as proposed in the previous paper [8]. Changes of $(K_I)_{est}$ and $(K_{II})_{est}$ with bent fatigue crack propagation are shown in Fig. 7. The values of $(K_I)_{est}$ for the fatigue slant precrack are smaller than those for the annealed slant precrack for both specimens with precracks of a slant angle β =60deg. and β =45deg. as shown in Fig. 7(a). Comparing the specimens with precrack of a slant angle β =60deg. and β =45deg., the values of $(K_I)_{est}$ obtained from the precrack with a slant angle of β =60deg. are larger for both the annealed slant precrack and fatigue slant precrack, corresponding to the fast crack propagation for the specimen with precracks of slant angle β =60deg. in spite of smaller applied stress conditions as indicated in Fig. 4. On the other hand, the values of $(K_{II})_{est}$ are almost zero except for the specimen with a fatigue precrack of slant angle β =45deg.. Although the values of $(K_{II})_{est}$ decrease with the bent fatigue crack propagation and become almost zero at a' 0.6 mm, the bent fatigue crack propagates under the mixed-mode condition immediately after the bent fatigue crack initiation from the fatigue precrack with slant angle of β =45deg..

4. DISCUSSIONS

4.1 Finite element method (FEM) analysis

In order to investigate the effects of the compressive residual stress along the slant precrack on the bent fatigue

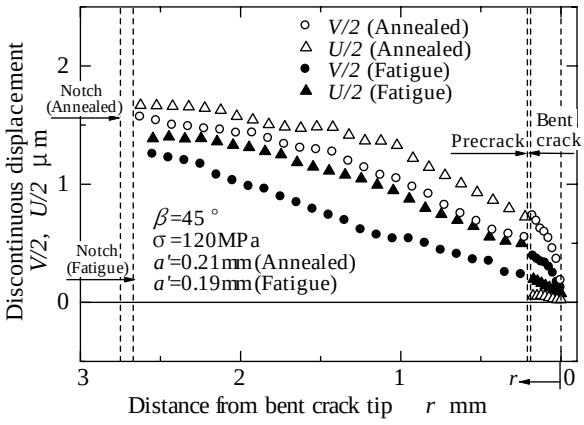

(a) β =45deg.

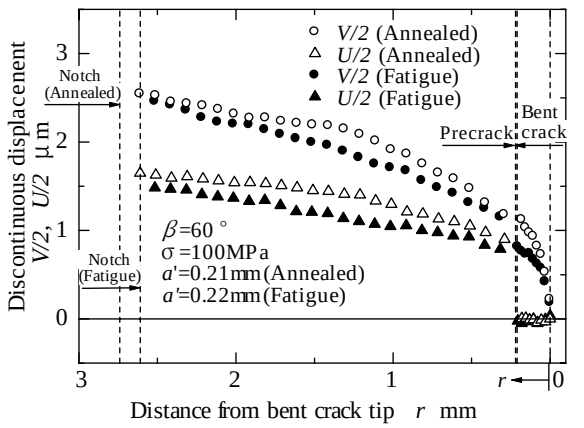

(b) β =60deg.

Fig. 6 Discontinuous displacement measured along precracks and bent fatigue cracks

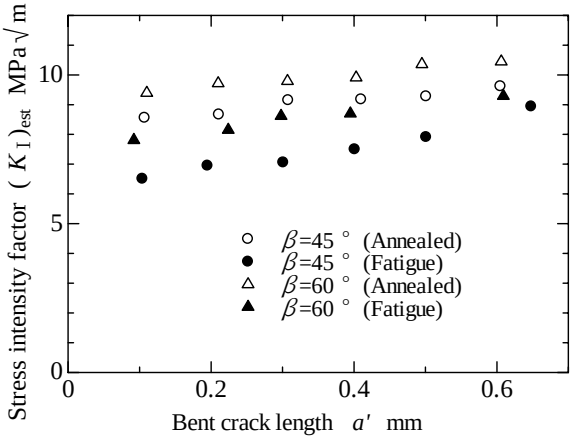

(a) Mode I

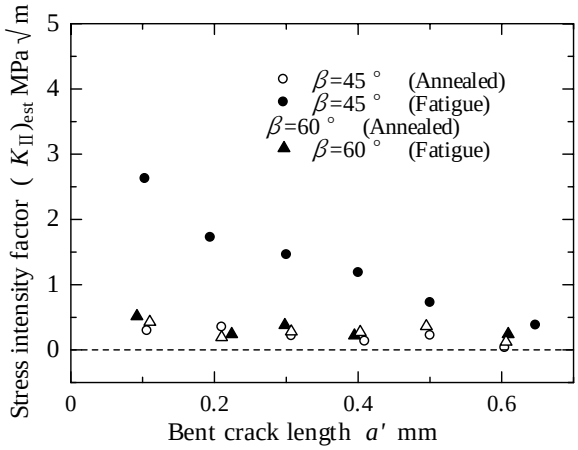

(b) Mode II

Fig. 7 Change of stress intensity factors with bent fatigue crack propagation

crack propagation rate and the fracture angle, discontinuous displacements were obtained for the specimen without the effects of the residual stress and the crack surface contact using a finite element method (FEM) analysis. Each FEM model of the specimen with a bent fatigue crack initiated from the slant crack containing the notch hole at the center was made based on the specimen used in the experiment as mentioned in section 2.1. The FEM model of the bent crack (a'=0.1mm) initiated from the precrack with a slant angle of β=45deg. under the tensile loading is shown in Fig. 8. The bent fatigue crack path in the FEM model was determined as the lines linked the points A, B and C explained in section 2.5. A four-nodes element was used in the analysis and the dimension of a minimum element around the bent crack tip was 0.01mm. The FEM analysis was calculated using the material constants, E=205.8GPa for Young's modulus and ν=0.3 for Poisson's ratio under the two-dimensional elastic plane stress condition. The applied stresses were σ=100MPa for the specimen with a precrack of slant angle β=60deg. and σ=120MPa for the specimen with a precrack of slant angle β=45deg. to the longitudinal direction according to each value of maximum stress in the bent fatigue crack propagation test. The finite element code used in the analysis was Marc K6.1.

Using the crack opening displacement and the crack sliding displacement obtained by the FEM analysis, Mode I and mode II stress intensity factors, $(K_I)_{FEM}$ and $(K_{II})_{FEM}$, were calculated using the displacement extrapolation method in the same way as mentioned in section 3.5.

4.2 Evaluation of the fracture angle

Substituting the $(K_I)_{est}$ and $(K_{II})_{est}$ calculated from the experimental discontinuous displacements and $(K_I)_{FEM}$ and $(K_{II})_{FEM}$ calculated from those obtained by FEM analysis for K_I and K_{II} in Eq. (2), fracture angles, θ_{est} and θ_{FEM} were estimated by the maximum tangential stress criterion [10].

$$K_I \sin\theta + K_{II}(3\cos\theta - 1) = 0 \qquad (2)$$

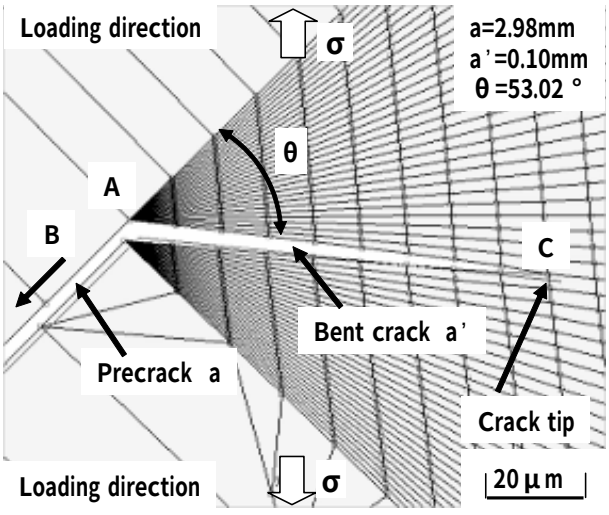

Fig. 8 FEM model of bent crack propagation from slant precrack (β=45deg.)

Table 1 shows the estimated fracture angles, θ_{est} and θ_{FEM}, obtained for the various bent fatigue cracks, comparing with the measured fracture angle, θ_{mes}, at the bent fatigue crack length of a'=0.10mm. Because the bent fatigue crack was propagated under a stress ratio of R=0 in this study, $(K_I)_{FEM}$ and $(K_{II})_{FEM}$ are equivalent to ΔK_I and ΔK_{II} determined only by a stress amplitude. As shown in Table 1, the differences between θ_{est} and θ_{FEM} do not exceed 1.5deg. and the values of θ_{est} and θ_{FEM} are almost equivalent to those of the measured fracture angle, θ_{mes}, except the fracture angles obtained from the fatigue precrack with a slant angle β=45deg.. For the specimen with fatigue precrack with a slant angle β=45deg., the differences between θ_{est} and θ_{FEM} are relatively large and the value of θ_{est} is closer to that of θ_{mes} than θ_{FEM}. As the values of θ_{est} calculated by substituting $(K_I)_{est}$ and $(K_{II})_{est}$ obtained from the experimental discontinuous displacements into Eq. (2) are almost equal to the values of the measured fracture angle, θ_{mes} for all precracks, the estimation of the fracture angle based on the maximum tangential stress criterion seems appropriately in this study like previous studies [1, 4].

Similarly, using $(K_I)_{est}$ and $(K_{II})_{est}$, $(K_I)_{FEM}$ and $(K_{II})_{FEM}$ obtained at every 100 μm bent crack propagation, the estimated fracture angles, θ_{est} and θ_{FEM}, were calculated from Eq. (2) at each bent crack length. The differences between the estimated fracture angles and measured angles, (θ_{est} - θ_{mes}) and (θ_{FEM} - θ_{mes}) are indicated in Fig. 9. The values of (θ_{est} - θ_{mes}) and (θ_{FEM} - θ_{mes}) obtained from all specimens except the value of (θ_{FEM} - θ_{mes}) obtained from the fatigue precrack of slant angle β=45deg. are almost zero during the bent fatigue crack propagation. As shown in Fig. 7, the other bent fatigue cracks except that initiated from the fatigue precrack with slant angle β=45deg. propagated under the mode I condition immediately after the bent fatigue crack initiation, while Kitagawa et. al. have reported the similar bent fatigue crack propagation behavior without mode II component [1]. On the other hand, it is necessary to use $(K_I)_{est}$ and $(K_{II})_{est}$ for estimating the fracture angle by the maximum tangential stress criterion under the mixed-mode condition containing the mode II component, which is probably caused by the crack surface contact on the slant precrack.

4.3 Evaluation of the stress intensity factor for the bent crack

The differences between the stress intensity factors evaluated from the experimental discontinuous displacement and those evaluated from the discontinuous dis-

Table 1 The measured and estimated fracture angles of bent fatigue crack

	Annealed			Fatigue		
	θ_{mes}°	θ_{est}°	θ_{FEM}°	θ_{mes}°	θ_{est}°	θ_{FEM}°
β=45°	52.44	51.95	50.78	53.98	54.81	50.62
β=60°	38.79	37.94	36.71	39.12	38.25	36.94

placements obtained by the FEM analysis, $\{(K_I)_{est}-(K_I)_{FEM}\}$ and $\{(K_{II})_{est}-(K_{II})_{FEM}\}$, which are the parameters suppressing the bent crack opening and sliding, were obtained. The changes of $\{(K_I)_{est}-(K_I)_{FEM}\}$ and $\{(K_{II})_{est}-(K_{II})_{FEM}\}$ with the bent fatigue crack propagation are indicated in Fig. 10. When the values of $\{(K_I)_{est}-(K_I)_{FEM}\}$ and $\{(K_{II})_{est}-(K_{II})_{FEM}\}$ are negative, the bent crack opening and sliding are suppressed. As the values of $\{(K_I)_{est}-(K_I)_{FEM}\}$ and $\{(K_{II})_{est}-(K_{II})_{FEM}\}$ obtained from the specimen with the annealed precrack with slant angle of β =60deg. and β =45deg. are almost zero, the stress intensity factors, $(K_I)_{est}$ and $(K_{II})_{est}$, evaluated from the experimental discontinuous displacement measured along the slant precrack and the bent fatigue crack using a displacement extrapolation method seem to be almost appropriate in this study. For the case of the specimen with the fatigue precrack, the values of $\{(K_{II})_{est}-(K_{II})_{FEM}\}$ are nearly zero for the bent fatigue crack initiated from the precrack with a slant angle of β =60deg., while the values of $\{(K_I)_{est}-(K_I)_{FEM}\}$ are a little negative. On the other hand, the values of $\{(K_I)_{est}-(K_I)_{FEM}\}$ obtained from the bent fatigue crack initiated from the fatigue precrack with slant angle β =45deg. show relatively large negative values and draw toward zero values with the bent fatigue crack propagation at the same as the values of $\{(K_{II})_{est}-(K_{II})_{FEM}\}$ decrease. Namely, the mode I component for the bent fatigue crack propagation seems to be suppressed immediately after the bent fatigue crack initiation, while the mode II component seems to be promoted. However, the bent fatigue crack becomes to propagate only under the mode I condition with the bent fatigue crack growth.

4.4 Bent fatigue crack propagation rate

The bent fatigue crack propagation rates, *da'*/*dN*, are plotted against the mode I stress intensity factors, $(K_I)_{est}$, as shown in Fig. 11. The dashed line shows the result of the approximation calculated by the least-squares fitting using all data and the correlation factor is 0.932. The solid line shows the result calculated using the data except those for the bent fatigue crack initiated from the fatigue precrack with a slant angle β =45deg., which is propagated with

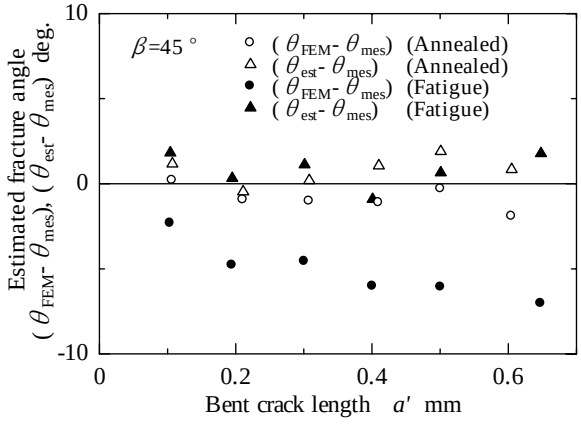

(a) β =45deg.

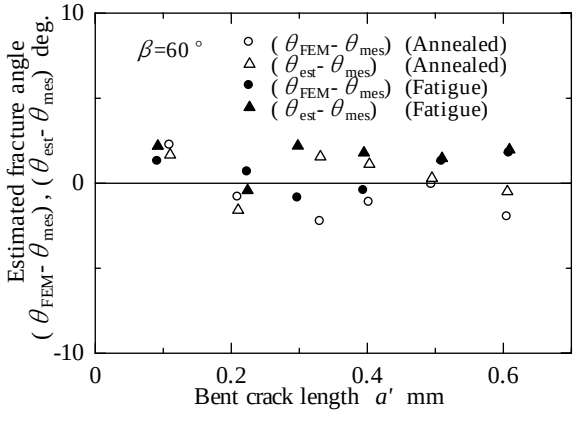

(b) β =60deg.

Fig. 9 Relationship between the estimated and the measured fracture angles during bent fatigue crack propagation

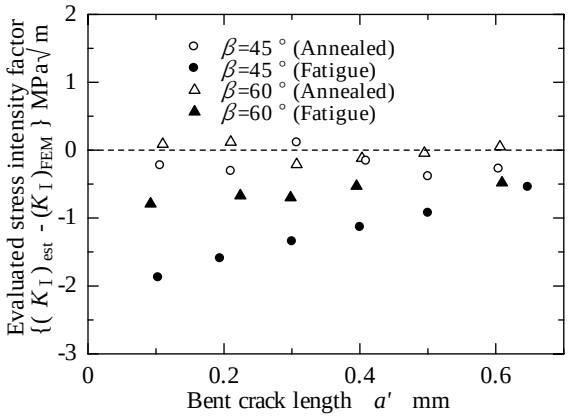

(a) Mode I

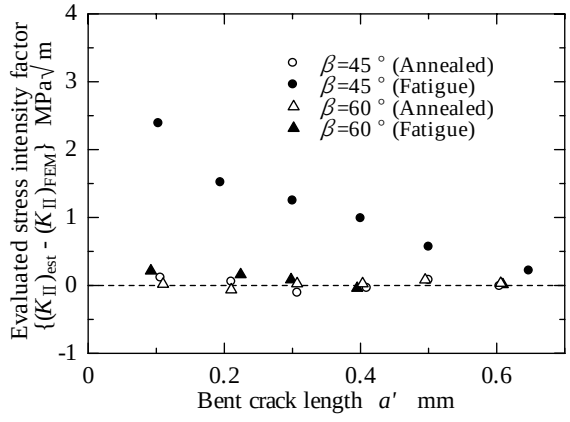

(b) Mode II

Fig. 10 The diffefence between the FEM calculated and the measured stress intensity factors during bent fatigue crack propagation

relatively large mode II components. On the other hand, mixed-mode stress intensity factor, $(K_M)_{est}$, is able to be evaluated from Eq. (3) using not only $(K_I)_{est}$ but also $(K_{II})_{est}$, as reported in the previous paper [11].

$$K_M = \left[K_I^4 + 8K_{II}^4 - \frac{2K_I^4 \times 8K_{II}^4}{\sqrt{\left(K_I^4\right)^2 + \left(8K_{II}^4\right)^2} + K_I^4 + 8K_{II}^4} \right]^{1/4} \quad (3)$$

The relationship between the bent fatigue crack propagation rates, *da'/dN*, and the mixed-mode stress intensity factors, $(K_M)_{est}$, is indicated in Fig. 12. The solid line shows the result calculated using all data and the correlation factor is 0.961. Since the correlation factor calculated using $(K_M)_{est}$ is larger than that using $(K_I)_{est}$, the relationship between *da'/dN* and $(K_M)_{est}$ seems to be fitted by one line including the results of the bent fatigue crack initiated from the fatigue precrack with a slant angle β =45deg.. However, the correlation factor obtained from the relationship between *da'/dN* and $(K_I)_{est}$ calculated using the data except those for the bent fatigue crack initiated from the fatigue precrack with a slant angle β =45deg. shows the sufficiently large value of 0.966. Therefore, the bent fatigue crack propagation rate without the mode II component is able to be evaluated only using the mode I stress intensity factor, $(K_I)_{est,}$ while the bent fatigue crack propagation rate under the mixed-mode condition containing the mode II component is necessary to be evaluated using the mixed-mode stress intensity factor, $(K_M)_{est}$.

5. CONCLUSIONS

In this study, bent fatigue crack propagation behaviors were discussed based on the discontinuous displacement distributions measured along a bent fatigue crack and a precrack with a slant angle of 60deg. and 45deg., noting a crack-surface contact due to a compressive residual stress around precracks. The main results obtained in this study are as follows :

(1) Mode I and mode II stress intensity factors, $(K_I)_{est}$ and $(K_{II})_{est}$, were calculated using the discontinuous displacements, which is the crack opening and sliding displacement, along bent fatigue cracks initiated from slant precracks. Since the stress intensity factors obtained from the bent fatigue cracks initiated from annealed slant precracks without compressive residual stress were in agreement with those obtained from the results calculated by the FEM analysis simulated the experimental results, the method of evaluating the stress intensity factor using the discontinuous displacement was probably appropriate in this study.

(2) The estimated fracture angles, θ_{FEM}, calculated by a maximum tangential criterion using the stress intensity factors, $(K_I)_{FEM}$ and $(K_{II})_{FEM}$ obtained from the FEM analysis were in good agreement with the measured fracture angle, θ_{mes}, for the bent fatigue crack propagation without the mode II component. On the other hand, the estimated fracture angles, θ_{est} , calculated using $(K_I)_{est}$ and $(K_{II})_{est}$ evaluated from the measured discontinuous displacements corresponded to θ_{mes} even for the bent fatigue crack propagation under the mixed-mode condition containing the mode II component, which is probably caused by the crack surface contact on the slant precrack.

(3) The bent fatigue crack propagation rate without the mode II component was able to be evaluated only using the mode I stress intensity factor, $(K_I)_{est,}$. On the other hand, the bent fatigue crack propagation rate under the mixed-mode condition containing the mode II component was necessary to be evaluated using the mixed-mode stress intensity factor, $(K_M)_{est}$ as the bent fatigue crack propagation rate was accelerated by the mode II component.

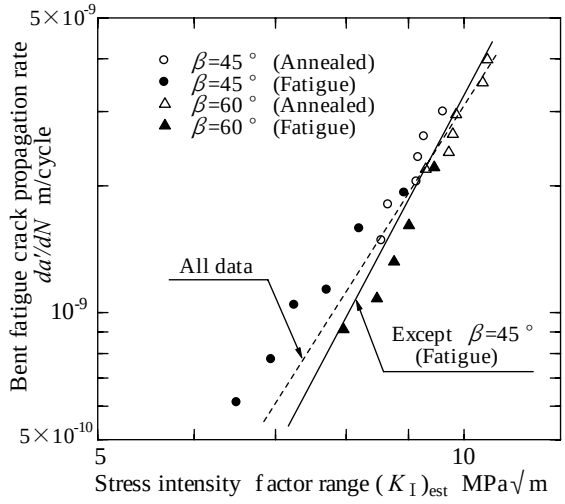

Fig. 11 Relationship between bent fatigue crack propagation rate and mode I stress intensity factor range $(K_I)_{est}$

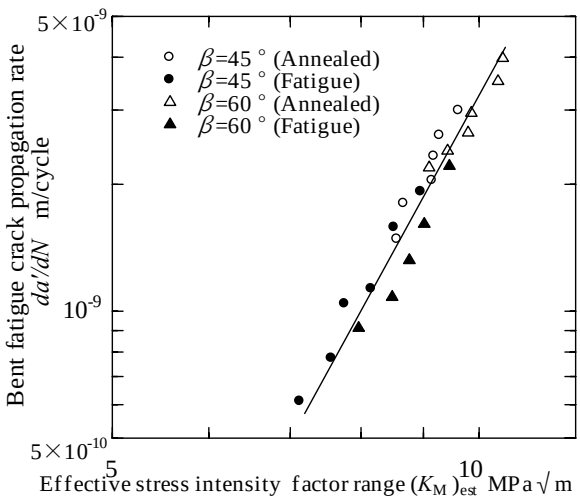

Fig. 12 Relationship between bent fatigue crack propagation rate and mixed-mode stress intensity factor range $(K_M)_{est}$

REFERENCES

[1] H. Kitagawa, R. Yuuki and K. Tohgo, Trans. Jpn. Soc. Mech. Eng., **47**-424 A(1981), 1283-1292.

[2] G. C. Sih, Eng. Fract. Mech., **13**(1980), 439-451.

[3] T. Yokobori, T. Yokobori, K. Ishii, K. Sato and K. Shyoji, J. Soc. Mat. Sci., **35**-395 (1986), 930-935.

[4] K. Ohji, M. Tsuji, S. Kubo, Y. Ono, A. Yahata and K. Umei, Trans. Jpn. Soc. Mech. Eng., **59**-562 A(1993), 1429-1436.

[5] H. Feng, J. Zhang and J. Rohde, Eng. Fract. Mech., **36**-6 (1990), 971-978.

[6] T. Torii, K. Honda and Y. Yoshimura, JSME Int. J., Ser. A, **37**-1 (1994), 14-21.

[7] K. Shimizu, Y. Ma and T. Torii, Trans. Jpn. Soc. Mech. Eng., **71**-709 A(2005), 1207-1212.

[8] T. Torii and K. Honda, K., J. Soc. Mat. Sci., **42**-476 (1993), 568-573.

[9] For example, H. Okamura: Introduction to Linear Fracture Mechanics, Baifukan (1990), 24-30.

[10] K. Ohji, T. Tsujikami and K. Hiraoka, J. Soc. Mat. Sci., **49**-8 (2000), 879-884.

[11] T. Torii, N. Toi and T. Tamura, JSME, Int. Journal Ser. A., **40**-3 (1997), 255-262.